

Quantum-mechanical calculation of Stark widths of Ne VII $n=3$, $\Delta n=0$ transitions

Yuri V. Ralchenko*

Department of Particle Physics, Weizmann Institute of Science, Rehovot 76100, Israel

Hans R. Griem†

Institute for Plasma Research, University of Maryland, College Park, Maryland 20742

Igor Bray‡ and Dmitry V. Fursa§

Electronic Structure of Materials Centre, School of Physical Sciences, The Flinders University of South Australia, G.P.O. Box 2100, Adelaide 5001, Australia

(Received 1 September 1998)

The Stark widths of the Ne VII $2s3s$ - $2s3p$ singlet and triplet lines are calculated in the impact approximation using quantum-mechanical convergent close-coupling and Coulomb-Born-exchange approximations. It is shown that the contribution from inelastic collisions to the linewidths exceeds the elastic width contribution by about an order of magnitude. Comparison with the linewidths measured in a hot dense plasma of a gas-liner pinch indicates a significant difference which may be naturally explained by nonthermal Doppler effects from persistent implosion velocities or turbulence developed during the pinch implosion. Contributions to the linewidth from different partial waves and types of interactions are discussed as well. [S1050-2947(99)03203-5]

PACS number(s): 32.70.Jz, 34.80.Kw, 52.55.Ez

I. INTRODUCTION

Spectral line shapes can provide very rich and valuable information on important plasma parameters, such as ion and atom temperature, electron density, electric field distributions, etc. The quantum-mechanical theory of collisional impact line broadening is well established and developed [1], however the number of purely quantum calculations, especially for highly charged ions, is rather limited. Most theoretical efforts were directed toward elaboration of semiclassical or semiempirical methods which showed good accuracy for neutral species and low-charge ions. It is only recently, when a number of sophisticated atomic collisional codes have become available, that high-quality quantum-mechanical results could be applied to line-shape calculations for highly charged ions. From the experimental point of view, test measurements of line profiles are impeded by the required independent determination of plasma temperature and density. The experimental situation is even more peculiar in that the linewidths of high- Z ions were measured almost exclusively by the Bochum group (see [2,3] and references therein), and therefore lack an independent confirmation.

The recent results on the Stark broadening of spectral lines from multiply charged ions revealed a significant discrepancy between the independent quantum-mechanical calculations and, on the other hand, experimental measurements and semiclassical results. For the B III measurements [4,5], the Stark linewidths for the simplest $2s$ - $2p$ transition differ by as much as a factor of 2, the two quantum results [6,7]

being in agreement to within 10%. A possible explanation for this discrepancy in terms of a developed turbulence and different treatments of small partial waves in electron-ion scattering was proposed in Ref. [6]; however, more comparisons and detailed investigation of important contributions to the linewidth are of primary importance.

Measurements of line profiles for the $2s3s$ - $2s3p$ transitions 1S_0 - 1P_1 and 3S_1 - 3P_2 of Ne VII emitted from a hot dense plasma of a gas-liner pinch were reported recently [3,8]. The experimental linewidths for singlet ($\lambda^S = 3643.6 \text{ \AA}$) and (the strongest) triplet ($\lambda^T = 1982.0 \text{ \AA}$) lines are $\Delta\lambda^S = 1.70 \pm 0.26 \text{ \AA}$ and $\Delta\lambda^T = 0.45 \pm 0.07 \text{ \AA}$, respectively. The electron density and temperature were measured *independently* by laser Thomson scattering and turned out to be in the ranges $N_e = (3-3.5) \times 10^{18} \text{ cm}^{-3}$ and $T_e = (19-20.5) \text{ eV}$. The measured linewidths agree well with most semiclassical [1,5,9] or semiempirical [10] calculations but only marginally with other semiempirical results [11].

Here we present the results of fully quantum-mechanical calculations of the Stark linewidths for the $n=3 \rightarrow 3$ transitions in Be-like neon. The plan of this paper is as follows. In Sec. II the calculational method is described. The features of atomic structure as well as inelastic and elastic contributions to the linewidths are discussed in detail. In Sec. III a comparison with available experimental and theoretical results is made and the sources of discrepancy are investigated. Finally, Sec. IV contains conclusions and recommendations.

II. METHOD

A. General theory

The calculational method applied here is basically the same as the one used in Ref. [6]. We start from the funda-

*Electronic address: fnralch@plasma-gate.weizmann.ac.il

†Electronic address: griem@glue.umd.edu

‡Electronic address: igor@yin.ph.flinders.edu.au

§Electronic address: dmitry@yin.ph.flinders.edu.au

mental formula for the full collisional width at half-maximum (FWHM) for an isolated line corresponding to a transition $u \rightarrow l$ [12]:

$$w = N_e \int_0^\infty v F(v) \left(\sum_{u' \neq u} \sigma_{uu'}(v) + \sum_{l' \neq l} \sigma_{ll'}(v) + \int |f_u(\theta, v) - f_l(\theta, v)|^2 d\Omega \right) dv, \quad (1)$$

with N_e being the electron density, v the velocity of the scattered electron, and $F(v)$ the Maxwellian electron velocity distribution. The electron impact cross sections $\sigma_{uu'}$ ($\sigma_{ll'}$) represent contributions from transitions connecting the upper (lower) level with other perturbing levels indicated by primes. In Eq. (1), the $f_u(\theta, v)$ and $f_l(\theta, v)$ are elastic scattering amplitudes for the target ion in the upper and lower states, respectively, and the integral is performed over the scattering angle θ , with $d\Omega$ being the element of solid angle. Equation (1) relates a linewidth in the impact approximation with atomic cross sections, facilitating the use of well-developed techniques of atomic scattering calculations for line broadening studies. It can also be rewritten in terms of the elastic \mathbf{S} -matrix elements assuming LS coupling (see, e.g., [13]):

$$w = \text{Re} \left(2\pi N_e \sum_{L_u^T L_l^T S^T l l'} (-1)^{l+l'} (2L_u^T + 1)(2L_l^T + 1) \times \frac{(2S^T + 1)}{2(2S + 1)} \begin{Bmatrix} L_l^T & L_u^T & 1 \\ L_u & L_l & l \end{Bmatrix} \begin{Bmatrix} L_l^T & L_u^T & 1 \\ L_u & L_l & l' \end{Bmatrix} \times \int_0^\infty \frac{1}{v} F(v) dv [\delta_{l'l} - S_U(L_u S l' \frac{1}{2} L_u^T S^T; L_u S l \frac{1}{2} L_u^T S^T) \times S_L^*(L_l S l' \frac{1}{2} L_l^T S^T; L_l S l \frac{1}{2} L_l^T S^T)] \right). \quad (2)$$

Here L and S are the atomic orbital angular momentum and spin, l and l' are the electron orbital angular momentum before and after collision, superscript T denotes the quantum numbers of the total electron+ion system, and the $\left\{ \begin{smallmatrix} a & b & c \\ d & e & f \end{smallmatrix} \right\}$ are 6-j symbols. The advantage of Eq. (1) is that it gives more clear insight as to the importance of inelastic and elastic contributions to the linewidth; therefore, we will mainly be referring to Eq. (1) in what follows.

In the present work, the inelastic cross sections appearing in Eq. (1) were calculated with two independent methods, i.e., the convergent close-coupling (CCC) and Coulomb-Born-exchange (CBE) approximations. The basic idea of the CCC method [14] lies in the close-coupling expansion with a large number of square-integrable states. A set of coupled Lippmann-Schwinger equations for the transition matrix is solved in momentum space, and the convergence of the results may be checked easily by increasing the number of the basis functions. The details of the CCC method can be found in a number of recent reviews [15,16], where a very good agreement with various experimental collisional data is shown. For the calculations with the more traditional CBE approximation, we made use of the code ATOM described in

Ref. [17]. In addition to the Coulomb attraction between ion and electron and exchange, ATOM accounts for normalization (unitarization) effects and uses experimental level energies when calculating the atomic wave functions and collisional cross sections. It is well known that the Coulomb-Born approximation corresponds to perturbation theory with $1/Z$ as expansion parameter, where Z is the spectroscopic charge; therefore, one can expect better accuracy for the CBE method applied to *highly charged* ions. Although the CCC method generally provides a superior accuracy, the use of ATOM greatly reduces the computational efforts. Comparison of CCC and CBE cross sections for highly charged H- and Li-like ions ($Z \lesssim 12$) demonstrated an excellent agreement between these two methods and available experimental data [18].

B. Atomic structure

Before proceeding to the details of collisional calculations, it is worth mentioning some features of the Ne VII atomic structure. First, the current version of the CCC code utilizes the Hartree-Fock (HF) frozen-core approximation for atomic wave functions. To study the validity of this approach, we have made a comparison of wave functions calculated with the full HF and HF frozen-core methods using the Cowan code [19]. The agreement between the two sets of wave functions proved to be very good, thereby justifying the use of the frozen-core approximation. These calculations were also used to determine the root-mean-squared radii of the lower $2s3s$ and upper $2s3p$ states, which were found to be $1.81a_0$ and $1.79a_0$, respectively, where $a_0 = 0.529 \times 10^{-8}$ cm is the Bohr radius. (Recall that the CBE ATOM code constructs atomic wave functions by solving the Schrödinger equation with *experimental* energies rather than solving *ab initio* HF equations.) Another measure indicating the level of accuracy are the oscillator strengths, which for the CCC calculations are found to agree within one percent with the Opacity Project results [20]. Since in some cases the *atom* oscillator strengths f_{ATOM} deviate from the high-accuracy results f_{acc} by as much as 15%, the CBE dipole-allowed excitation cross sections were rescaled by the ratio $f_{\text{acc}}/f_{\text{ATOM}}$ to improve these results. Finally, to check the applicability of LS coupling, we carried out large-scale atomic structure calculations for Ne VII with Cowan's code taking into account both intermediate coupling and configuration interaction. The results obtained show that the levels of interest of Ne VII correspond to practically pure LS coupling, although configuration interaction is important for the $2s3p^1P$ and $2p3s^1P$ states which mix to a level of 10%. Nonetheless, this mixture is unlikely to be important, since in the sum of inelastic cross sections in Eq. (1) this effect is essentially smoothed out.

C. Inelastic collisions

The inelastic cross sections appearing in Eq. (1) include all possible electron-induced transitions originating from the lower or upper states of a transition. It is normally safe to neglect the ionization and recombination processes, taking into account only electron impact excitation and deexcitation. For the linewidths discussed here, even the $\Delta n \neq 0$ excitations may (but will not) be ignored, since their rates are

TABLE I. The CBE electron impact excitation and deexcitation rate coefficients for Ne VII in units of $\text{cm}^3 \text{s}^{-1}$ for $T_e = 20 \text{ eV}$. The numbers in brackets denote powers of 10.

	$2s3s\ ^3S$	$2s3s\ ^1S$	$2s3p\ ^1P$	$2s3p\ ^3P$
$2s3s\ ^3S$		7.46[−10]	3.29[−10]	6.10[−08]
$2s3s\ ^1S$	2.21[−10]		5.17[−08]	1.13[−10]
$2s3p\ ^1P$	2.47[−10]	1.31[−07]		5.30[−10]
$2s3p\ ^3P$	1.35[−07]	8.44[−10]	1.56[−09]	
$2s3d\ ^3D$	9.96[−09]	1.50[−09]	1.48[−09]	7.75[−08]
$2s3d\ ^1D$	4.10[−10]	9.97[−09]	6.45[−08]	4.49[−10]
$2p3s\ ^3P$	9.71[−09]	3.86[−10]		
$2p3s\ ^1P$	9.99[−11]	2.36[−08]		
$2p3p\ ^1P$			1.20[−08]	4.34[−11]
$2p3p\ ^3D$			2.04[−10]	9.69[−09]
$2p3p\ ^3S$			3.89[−11]	2.18[−09]
$2p3p\ ^3P$			1.12[−10]	3.86[−09]
$2p3p\ ^1D$			7.04[−10]	5.92[−11]
$2p3p\ ^1S$			6.63[−10]	1.07[−11]

at least two orders of magnitude smaller than those for the $\Delta n = 0$ transitions. Table I presents the CBE rate coefficients for electron impact excitation and deexcitation processes connecting the upper and lower levels of transitions with other perturbing $2l3l'$ levels. The calculation was carried out for an electron temperature $T_e = 20 \text{ eV}$, which corresponds to the experimental conditions of Ref. [8], and only one-electron transitions are considered here since two-electron transitions were found to have much smaller cross sections. One can see that the largest rate coefficients correspond to dipole-allowed transitions, while dipole-forbidden and spin-forbidden channels contribute only a few percent to the inelastic part of the linewidth. It should also be noted that since the reaction thresholds are smaller than 6–7 eV, the rate coefficients are rather insensitive to small (a few eV) variations in the electron temperature around the experimental value of 20 eV.

Both calculational methods give close (within 10%) results for the most important dipole-allowed cross sections. (Note that the excitation of the inner $2l$ electron is also significant for the linewidth, contributing as much as 12% and 8% for singlet and triplet lines, respectively.) An example of the agreement between the CCC and CBE results is demonstrated in Fig. 1, where $2s3s\ ^1S-2s3p\ ^1P$ and $2s3p\ ^3P-2s3d\ ^3D$ excitation cross sections are shown. Unfortunately, there are no other available theoretical nor experimental data for the 3-3 transitions in Ne VII, so in order to test the accuracy of our calculations it seems to be reasonable to make a comparison with the existing 2-3 data for this ion. Probably, the most accurate theoretical results were produced recently by Ramsbottom *et al.* [21], who calculated electron impact excitation rates for many 2-3 transitions using the multichannel R -matrix method. The comparison shows very good agreement between our data and those of Ref. [21]. For instance, the CBE excitation rate coefficients ($T_e = 10^6 \text{ K} \approx 86 \text{ eV}$) for the outer electron transition $2s2p\ ^3P-2s3d\ ^3D$ and inner electron transition $2s2p\ ^3P-2p3s\ ^3P$ are $6.8 \times 10^{-10} \text{ cm}^3 \text{ s}^{-1}$ and $9.1 \times 10^{-11} \text{ cm}^3 \text{ s}^{-1}$, respectively, which agree well with the

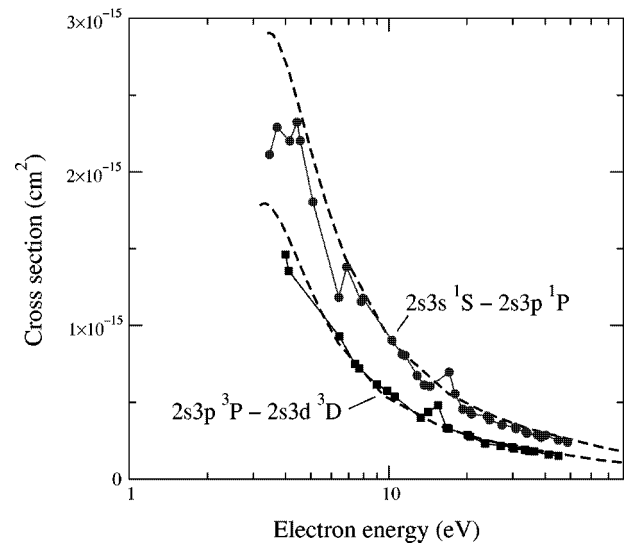


FIG. 1. Electron impact excitation cross sections for the transitions $2s3s\ ^1S-2s3p\ ^1P$ and $2s3p\ ^3P-2s3d\ ^3D$ in Ne VII. CBE, dashed lines; CCC, solid circles and squares.

R -matrix values of 6.2×10^{-10} and $9.6 \times 10^{-11} \text{ cm}^3 \text{ s}^{-1}$. There also exist θ -pinch experimental results [22] for excitation rates from the ground and metastable states to some of the $n=3$ states at an electron temperature of 260 eV; these are two to three times smaller than CCC/CBE rates, but large experimental errors up to 200–300% limit their usefulness.

To summarize, for the experimental conditions of Ref. [8], the CBE inelastic contribution (with account of the $\Delta n = 1$ transitions) to the linewidths obtained from Eq. (1) is $w_{in}^S \approx 0.806 \text{ \AA}$ for the singlet line and $w_{in}^T \approx 0.197 \text{ \AA}$ for the triplet line.

D. Elastic collisions

According to Eq. (1), the non-Coulomb elastic amplitudes of scattering from the upper and lower states at the same electron impact energy should be subtracted and averaged

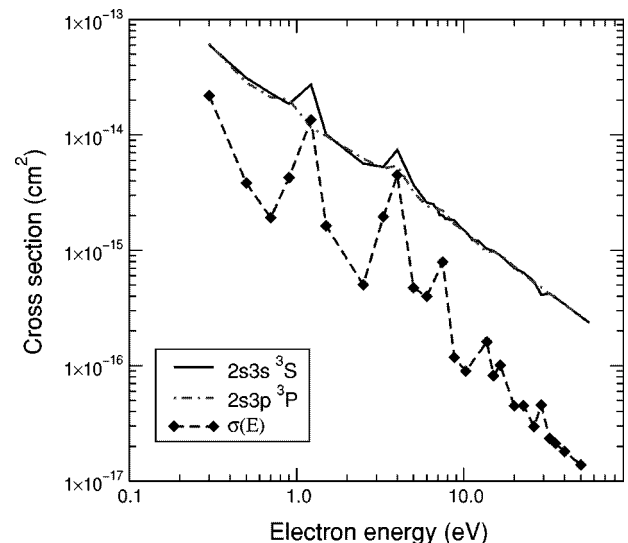


FIG. 2. Non-Coulomb elastic cross sections of Ne VII ions in $2s3s\ ^3S$ (solid line) and $2s3p\ ^3P$ (dot-dashed line) states, and the coherent difference term $\tilde{\sigma}(E)$ (diamonds).

TABLE II. Ratio of the experimental Stark widths of the $2s3s$ - $2s3p$ lines in Ne VII to different theoretical widths.

Line	T_e (eV)	N_e (cm $^{-3}$)	$w_{\text{expt}}/w_{\text{theor}}$				
Ne VII 1S_0 - 1P_1	19	3.5×10^{18}	1.28 ^a	1.15 ^b	1.57 ^c	0.88(0.77) ^d	1.70 ^e
Ne VII 3S_1 - 3P_2	20.5	3.0×10^{18}	1.53 ^a	1.29 ^b	1.91 ^c	0.94(0.82) ^d	1.96 ^e

^aSemiclassical [1].

^bSemiempirical [10].

^cSemiempirical [11].

^dSemiclassical [5].

^ePresent work.

over the Maxwellian electron energy distribution. These amplitudes were calculated for a large range of electron energies only with the CCC code, since the existing version of the CBE code ATOM produces only inelastic cross sections. The $2s3s$ 3S and $2s3p$ 3P elastic cross sections $\sigma_{\text{el}}(E)$ along with the coherent difference term $\tilde{\sigma}(E) \equiv \int |f_s(\theta, v) - f_p(\theta, v)|^2 d\Omega$ are shown in Fig. 2, the singlet cross sections and difference term having a similar behavior. These results unambiguously reveal the same peculiarities as were noticed for the B III $2s$ - $2p$ elastic term [6], i.e., a faster than $1/E$ energy dependence and strong cancellation in $\tilde{\sigma}(E)$. For example, at electron impact energies $E \geq 30$ eV, the coherent difference $\tilde{\sigma}$ is more than an order of magnitude smaller than any of the σ_{el} . Since at large energies the elastic cross section is mainly determined by the size of a system, such a cancellation may be due to almost equal mean squared radii of the $2s3s$ and $2s3p$ states, as was already mentioned above. The general behavior of the elastic difference term deserves a special investigation and will be reported elsewhere. The Maxwell-averaged elastic contribution to the linewidth is $w_{\text{el}}^S \approx 0.067$ Å and $w_{\text{el}}^T \approx 0.023$ Å for singlet and triplet, respectively. This shows that in this case the elastic contribution to the linewidths is about an order of magnitude smaller than the inelastic one, which is not surprising for such high temperatures.

E. Final results

To summarize, the total linewidths (FWHM) for the $2s3s$ - $2s3p$, 1S - 1P , and 3S - 3P transitions obtained from Eq. (1) are $w_1^S \approx 0.873$ Å and $w_1^T \approx 0.220$ Å. The same widths were also calculated with Eq. (2) using the CCC elastic \mathbf{T} -matrix elements and the relation between \mathbf{T} matrix and \mathbf{S} matrix $\hat{\mathbf{T}} = \hat{\mathbf{S}} - \hat{\mathbf{I}}$ ($\hat{\mathbf{I}}$ is the unit matrix). The corresponding singlet and triplet widths are $w_2^S \approx 1.05$ Å and $w_2^T \approx 0.230$ Å. The difference between the results obtained with Eqs. (1) and (2) can probably be attributed to the resonances in the CCC \mathbf{T} matrix, which were not included into the CBE inelastic calculations. A conservative estimate of the accuracy of these results, based on the CCC-CBE agreement and the accuracy of the CCC calculations along the [Be] sequence, is 15%. Thus, the final Stark linewidths are

$$w^S = 1.0 \pm 0.15 \text{ Å}, \quad w^T = 0.23 \pm 0.03 \text{ Å}. \quad (3)$$

III. DISCUSSION

The linewidths calculated here differ noticeably from the measured values of Ref. [8] and most of the theoretical data.

The ratios of experimental to different theoretical Stark widths for the Ne VII lines are presented in Table II. The methods cited there cover various modifications of the semiclassical [1,9] and semiempirical [10,11] approximations. The semiclassical methods, including the latest nonperturbative calculations [9], yield values which are generally in agreement with the experimental data. The semiempirical results of Dimitrijević and Konjević [11] are rather close to our values, and this is quite similar to what had already been noticed for the B III calculations [6].

The major diagnostics challenge in the gas-liner pinch experiment [8] may be the determination of the main plasma parameters, i.e., the electron temperature and density, in a region where the multiply charged ions of neon are situated. In the experiment, both T_e and N_e were determined from the Thomson scattering only *globally*, which may not be characteristic of the plasma conditions near the locally injected neon. As a matter of fact, there exist some experimental indications that density and temperature do vary in the vicinity of the doping gas [23]. However, the experimental value of T_e is supported by the fact that electron temperatures $T_e = 19$ – 20 eV are well within the range of the maximal abundance temperatures for Ne VII at an electron density $N_e = (3$ – $4) \times 10^{18}$ cm $^{-3}$. Our calculations with the collisional-radiative code NOMAD [24] show that for equilibrium conditions the Ne VII ions account for about 30% of the total amount of neon. Another line broadening mechanism affecting the observed widths may be unresolved Doppler line splitting associated with the radial implosion velocities in the gas-liner pinch [23]. The contribution from an ion (proton) collisional broadening may be estimated using Eq. (517) from Ref. [1], and it is easy to show that ion broadening is negligibly small comparing to electron impact broadening.

Since the experimental conditions in the Ne VII measurements were basically the same as for the B III experiment, the general conclusions [6] regarding a possible effect of a developed turbulence on the linewidths should remain essentially the same. It was mentioned in Ref. [8] that the measured value of the Stark width for the triplet transition $\Delta\lambda \approx 0.45$ Å constitutes about 70% of the total measured linewidth¹ which therefore is $\Delta\lambda_{\text{exp}} \sim 0.64$ Å. This full width includes Stark, Doppler, and instrumental broadening, the latter being decomposed into Gaussian (0.07 Å) and

¹There is no information in Ref. [8] on the full linewidth of the singlet transition, so we will not discuss it in what follows.

Lorentzian (0.05 Å) parts [2]. For an ion temperature of $T_i = T_e = 20$ eV, the pure Doppler width is approximately $\Delta\lambda_D \approx 0.15$ Å. As noted in [6], the Reynolds numbers for the Bochum gas-liner pinch experiment are of the order of 10^4 , which is sufficient for a developed turbulence to exist. Such a turbulence leads to an extra chaotic motion of Ne ions with a characteristic velocity of the order of the proton thermal velocity v_p . Hence, the full thermal+turbulent Doppler width becomes a factor $\sqrt{20+1} \approx 4.6$ larger (here 20 is the ratio of masses M_{Ne}/M_H) and is now $\Delta\lambda_D \approx 0.70$ Å. Using Eq. (6) of Ref. [25], for the FWHM of a combined Voigt profile including Stark, thermal+turbulent Doppler, and instrumental contributions, we get a value $\Delta\lambda \approx 0.85$ Å which is 30% higher than $\Delta\lambda_{exp}$. The main uncertainty in this calculation obviously comes from the turbulent contribution, which is rather sensitive to the value of the characteristic velocity. It is straightforward to show that reducing this velocity by one-third only, i.e., multiplying the pure Doppler width by 3.1 instead of 4.6, one can exactly reproduce the experimental value of $\Delta\lambda_{exp}$. Thus, according to the hypothesis proposed in Ref. [6], reasonable values of characteristic turbulent velocities may naturally explain the observed difference in linewidths.

Regarding the discrepancy between the quantum and other theoretical calculations, the reader may wonder as to the source of such a difference. The crucial point is that unlike the quantum-mechanical methods, the semiclassical approaches have a natural limit of applicability arising from the Heisenberg uncertainty principle (see, e.g., [26]). The criterion of applicability of the semiclassical calculations may be formulated [27] as a requirement for the distance of the closest approach r_{min} , rather than the impact parameter ρ , to be larger than or at least of the same order as the corresponding de Broglie wavelength, $\lambda_{min} = 2\pi\hbar/mv_{max}$. Using the angular momentum conservation, it is straightforward to show that this is equivalent to the inequality

$$2\pi\hbar \leq L. \quad (4)$$

Another limitation on impact parameters was introduced in order to avoid violations of unitarity [1], but still assuming the long-range dipole interaction remain valid. Again reformulated in terms of the distance of the closest approach, the corresponding condition may be written as

$$\frac{r_n}{r_{min}} \leq 1, \quad (5)$$

where r_n is the excited state atomic radius. If this inequality is violated, both semiclassical and long-range interaction approximations are questionable. Using the Coulomb parameter $\eta = (Z-1)e^2/\hbar v$, Eq. (5) may also be expressed in terms of the total angular momentum L as [27]

$$\frac{r_n}{r_{min}} = \frac{(Z-1)r_n\{[1+(L/\eta)^2]^{1/2}+1\}}{a_0 L^2} \leq 1. \quad (6)$$

As was noted above, the mean root squared radii of the $2s3s$ and $2s3p$ states are about $1.8a_0$. For $T_e = 20$ eV, the Coulomb parameter is $\eta \approx 7$ and therefore the ratio r_n/r_{min} takes values of 1.45, 0.96, 0.43, and 0.22 for $L = 4, 5, 8,$ and $12,$

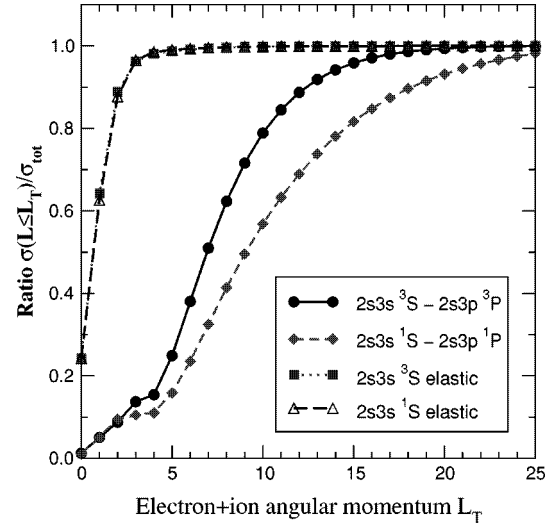


FIG. 3. Contribution of different total electron+ion angular momenta L_T to various elastic and inelastic cross sections.

respectively. It follows then that for the given electron temperature, criteria (4) and (5) are similarly restrictive for the semiclassical approximation.

Unlike in the semiclassical method, in fully quantum-mechanical calculations the determination of the range of significant L values is naturally accomplished by the partial wave expansion. In Fig. 3 the contribution of different total electron+ion angular momenta L_T to the CCC cross sections is shown for an incident electron impact energy of 20 eV for a number of transitions.² Naturally, the elastic cross sections are governed by the smallest values of L_T , which are concealed in the strong collision term of semiclassical calculations. The most important inelastic cross sections having the smallest thresholds reach 50% of their values only for $L = 9$, for which the left-hand side ratio of Eq. (5) is about 0.35. This number is probably already sufficiently small to justify the use of the long-range interaction approximation for $L \geq 9$; however, the restrictions following from Eq. (4) are less obvious to have been overcome.

Another discrepancy may come from other than dipole interactions. Although the monopole interaction was not explicitly included in nonperturbative semiclassical calculations [9], the quadrupole transition $2s3s-2s3d$ was shown to account for about 15% of the linewidth. This value is in contradiction with the present results. As one can see from Table I, the $2s3s-2s3d$ quadrupole channel contributes only approximately 3% to the quantum-mechanical inelastic linewidth. If we take into account only those transitions that were considered in Ref. [9], then this number increases to 3.5%, still a factor of 4 smaller than the nonperturbative semiclassical result.

These considerations clearly show that the accuracy of the semiclassical calculations may not be as high as it is often thought to be, and new calculations, both semiclassical and quantum-mechanical, are needed to better establish the limits of applicability for the nonquantum methods.

²The CBE partial wave composition is practically the same.

IV. CONCLUSION

A fully quantum-mechanical calculation of the Stark line-widths for the singlet and triplet $2s3s$ - $2s3p$ lines of Ne VII was carried out in the impact approximation with the use of accurate atomic data. Although the results obtained disagree with experimental and most theoretical results, a natural explanation for this disagreement can be suggested. On one hand, the measurements are not free from difficulties related to possible extra contributions from turbulence and unresolved Doppler shifts. This suggests an independent measurement of Stark widths of highly charged ions. On the other hand, the semiclassical calculations, not obviously pro-

ducing accurate results for other than dipole interactions, may have problems when being applied to the small impact parameter region. In our opinion, the next important step in the development of Stark broadening theory would be a very detailed comparison between quantum and semiclassical results.

ACKNOWLEDGMENTS

This work was supported in part by the Israeli Academy of Sciences and the Ministry of Sciences of Israel (Yu.V.R.), by the U.S. National Science Foundation (H.R.G.), and by the Australian Research Council (I.B. and D.V.F.).

-
- [1] H. R. Griem, *Spectral Line Broadening by Plasmas* (Academic, New York, 1974).
- [2] S. Glenzer, in *Atomic Processes in Plasmas*, edited by A. L. Osterheld and W. H. Goldstein, AIP Conf. Proc. No. 381 (AIP, Woodbury, NY, 1996), pp. 109–122.
- [3] Th. Wrubel, I. Ahmad, S. Büscher, H.-J. Kunze, and S. H. Glenzer, *Phys. Rev. E* **57**, 5972 (1998).
- [4] S. Glenzer and H.-J. Kunze, *Phys. Rev. A* **53**, 2225 (1996).
- [5] S. Alexiou, in *13th International Conference on Spectral Line Shapes*, edited by M. Zoppi and L. Ulivi, AIP Conf. Proc. No. 386 (AIP, Woodbury, NY, 1997), pp. 79–98.
- [6] H. R. Griem, Yu. V. Ralchenko, and I. Bray, *Phys. Rev. E* **56**, 7186 (1997).
- [7] M. J. Seaton, *J. Phys. B* **21**, 3033 (1988).
- [8] Th. Wrubel, S. Glenzer, S. Büscher, H.-J. Kunze, and S. Alexiou, *Astron. Astrophys.* **306**, 1023 (1996).
- [9] S. Alexiou, *Phys. Rev. Lett.* **75**, 3406 (1995).
- [10] J. D. Hey and P. Breger, *S. Afr. J. Phys.* **5**, 111 (1982).
- [11] M. S. Dimitrijević and N. Konjević, in *5th International Conference on Spectral Line Shapes*, edited by B. Wende (Walter de Gruyter, Berlin, 1981), pp. 211–239.
- [12] M. Baranger, *Phys. Rev.* **112**, 855 (1958).
- [13] G. Peach, in *Atomic, Molecular & Optical Physics Handbook*, edited by G. W. F. Drake (AIP, Woodbury, NY, 1996), Chap. 57.
- [14] I. Bray, *Phys. Rev. A* **49**, 1066 (1994).
- [15] I. Bray and A. T. Stelbovics, *Adv. At., Mol., Opt. Phys.* **35**, 209 (1995).
- [16] D. V. Fursa and I. Bray, *J. Phys. B* **30**, 757 (1997).
- [17] V. P. Shevelko and L. A. Vainshtein, *Atomic Physics for Hot Plasmas* (IOP, Bristol, 1993).
- [18] V. I. Fisher, Yu. V. Ralchenko, V. A. Bernshtam, A. Goldgirsh, Y. Maron, H. Golten, L. A. Vainshtein, and I. Bray, *Phys. Rev. A* **55**, 329 (1997); V. I. Fisher, Yu. V. Ralchenko, V. A. Bernshtam, A. Goldgirsh, Y. Maron, L. A. Vainshtein, and I. Bray, *ibid.* **56**, 3726 (1997).
- [19] R. D. Cowan, *The Theory of Atomic Structure and Spectra* (University of California Press, Berkeley, 1981).
- [20] J. A. Tully, M. J. Seaton, and K. A. Berrington, *J. Phys. B* **23**, 3811 (1990).
- [21] C. A. Ramsbottom, K. A. Berrington, and K. L. Bell, *At. Data Nucl. Data Tables* **61**, 105 (1995).
- [22] W. D. Johnston and H.-J. Kunze, *Phys. Rev. A* **4**, 962 (1971).
- [23] H.-J. Kunze (private communication); see also S. Büscher, Th. Wrubel, I. Ahmad, and H.-J. Kunze, in *14th International Conference on Spectral Line Shapes*, AIP Conf. Proc. (AIP, Woodbury, NY, in press).
- [24] Yu. V. Ralchenko, V. I. Fisher, and Y. Maron (unpublished).
- [25] E. E. Whiting, *J. Quant. Spectrosc. Radiat. Transf.* **8**, 1379 (1968).
- [26] E. J. Williams, *Rev. Mod. Phys.* **17**, 217 (1945).
- [27] H. R. Griem, in *14th International Conference on Spectral Line Shapes*, AIP Conf. Proc. (AIP, Woodbury, NY, in press).